Received: 2 March 2023 | Accepted: 14 November 2023

DOI: 10.1002/2688-8319.12296

Ecological Solutions and Evidence | BRITISH ECOLOGICAL SOCIETY

RESEARCH ARTICLE

Assessment of peatland burning in Scotland during 1985–2022 using Landsat imagery

B. D. Spracklen | D. V. Spracklen

School of Earth and Environment, University of Leeds, Leeds, UK

Correspondence
B. D. Spracklen
Email: b10spracklen@gmail.com

Funding information
H2020 European Research Council, Grant/Award Number: 771492; Natural Environment Research Council, Grant/Award Number: NE/L013347/1

Handling Editor: Lukas Egarter Vigl

Abstract

1. In the Scottish uplands, prescribed burning of moorland vegetation is widely practised either to boost gamebird numbers for recreational shooting or to improve livestock grazing. In recent years, this system of land management has become controversial due to concerns over the potential impacts on ecosystem services. However, there are limited data on the extent, distribution or frequency of burning and it is unclear whether there are long-term trends in burning. Crucially, the extent of burning on peat soils is not well known.
2. We used a time series of Landsat imagery covering 7750 km^2 of moorland in Eastern Scotland to detect annual variation in area burnt from 1985 to 2022. Burnt areas were detected using annual changes in Normalised Burn Ratio.
3. An accuracy evaluation conducted over eight sites covering 415 km^2 using a combination of Google Earth imagery, and field studies suggested a user's accuracy of 90% and a producer's accuracy of 77%.
4. We estimate an average annual mean area burnt of 61 km^2 with large interannual variability and no significant change in area burnt over the 38-year study period. We estimate that 32% of burning (19 km^2 $year^{-1}$) occurred on deep peat soils with no reduction in burning on deep peat after the revision of national guidelines (the Muirburn Code) in 2017 recommended ceasing this practice.
5. We find that in Eastern Scotland there has been no significant change in moorland area burnt over the last four decades. The fractional area burnt that is on deep peat is a matter of management concern.

KEYWORDS
heather moorland, Landsat, peatland, prescribed burning

1 | INTRODUCTION

In the UK, large areas of peatland occur in upland areas covered by low-growing moorland vegetation (Holden et al., 2007). These upland areas provide a range of important environmental services including moderation of downstream flood risk and a water source for 70% of the UK's population (Martin-Ortega et al., 2014). The widespread occurrence of peatland soils means the UK uplands are a particularly important carbon store (Bain et al., 2011; Chapman et al., 2009), storing an estimated 5100 Mt of carbon (Smith et al., 2007).

Many upland areas in the UK are intensively managed for the recreational shooting of red grouse (*Lagopus lagopus scotica* Lath.) (Miller, 1980). Management includes prescribed burning (Worrall et al., 2010) to create a patchwork of young and old heather (*Calluna vulgaris*) and boost red grouse numbers (Thompson et al., 2016). Prescribed burning of moorland and peatland in the UK has become increasingly controversial (Brown & Holden, 2020) particularly due to potential impacts on ecosystem services (England & Glaves, 2013; Harper et al., 2018).

Peatland fires release large quantities of carbon dioxide (Friedlingstein et al., 2022). Prescribed burning can significantly reduce carbon sequestration of blanket bog (Garnett et al., 2000; Marrs et al., 2019) and reduce carbon stocks in surface peat (Ward et al., 2007). Burning also impacts peatland hydrology, downstream flood risk (Holden et al., 2014, 2015), erosion (Li et al., 2018) as well as macro-invertebrate diversity (Brown et al., 2013) and stream water quality (Clay et al., 2012; Ramchunder et al., 2013). Fires emit pollutants which impact air quality (Graham, Pope, McQuaid, et al., 2020; Graham, Pope, Pringle, et al., 2020). Burning also impacts vegetation composition (Noble et al., 2018, 2019) and prevents the natural succession of vegetation (Fuller & Calladine, 2014).

Advocates of prescribed burning note the biodiversity value of managed grouse moors, particularly with regard to bird species such as the Eurasian curlew (*Numenius arquata*; Baines et al., 2008; Newey et al., 2016; Tharme et al., 2001), though this value has been attributed to stringent predator control rather than to the burning regime (Littlewood et al., 2019; Ludwig et al., 2019). It is further argued that alternative land uses to grouse shooting such as afforestation or conversion to farmland would damage biodiversity, although this narrative has recently been questioned (Crowle et al., 2022). Management for grouse has been seen as an important factor in maintaining heather moorland (Robertson et al., 2001). There is a complex relationship between prescribed burning and wildfire risk; although prescribed burns can reduce wildfire risk in heather-dominated moorlands, prescribed burns increase the dominance of fire-prone heather vegetation over blanket bog vegetation that is less easily burned (Worrall et al., 2010) potentially maintaining and exacerbating a fire-prone environment.

Scotland contains 88% of the UK's peatland carbon store due to the widespread extent of peatlands (Smith et al., 2007). In Scotland, prescribed burning is known as 'muirburn' and the 'Muirburn Code' (https://www.nature.scot/muirburn-code) provides advice and guidance on moorland burning. Muirburn is permitted between 1 October and 30 April inclusive, though burning in the latter half of April is not recommended. Land managers are advised to restrict burning to small areas, with a width of less than 30 m and to avoid burning steep slopes or close to water courses. The revised 2017 code also recommends against the use of burning on peatland. Burning within a Site of Special Scientific Interest (SSSI) may require permission from Scottish Natural Heritage (SNH) in some circumstances.

Despite the potential impacts of prescribed burning on numerous important environmental services, there have been few previous studies on the extent of burning in the UK. Little is known about how much burning occurs on peat or whether the amount of burning has changed in recent years (Harper et al., 2018). Aerial photographs have been used to assess burning over limited regions of England (Yallop et al., 2006). Hester and Sydes (1992) used historic aerial photography from the 1940s, 1960s and 1980s to detect changes in burning at 32 sites in the Grampian Mountains and Southern Uplands. Douglas et al. (2016) also used aerial photography in combination with MODIS satellite imagery to detect burning in UK moorland areas from 2001 to 2011, reporting an increasing number of fires over that period. A follow-up study in 2018 likewise used aerial photography and high-resolution satellite imagery to map burn distribution in Scotland (Matthews et al., 2020).

Coarse spatial resolution satellite data (250 m to 1 km) are now routinely used to map burnt area (Vetrita et al., 2021). However, the spatial resolution of these products is too coarse to detect small prescribed burns. More recently, higher resolution Landsat (30-m resolution) and Sentinel-2 (10–20 m) imagery has been exploited to identify and map small and fragmented burns that are not identified in lower resolution imagery (Boschetti et al., 2015; Gaveau et al., 2021; Ramo et al., 2021; Roteta et al., 2019, 2021; Roy et al., 2019). However, to date this higher resolution imagery has not been widely used to quantify burn extent across the UK.

Here, we use Landsat imagery to detect burnt area across upland areas of Scotland over the period 1985–2022. The temporal and spatial resolution of Landsat combined with its unbroken decades-long image archive enables us to detect small burns and to produce annual estimates of burnt area based on postfire changes in vegetation. Our study aims to quantify the annual extent and distribution of muirburn in Scotland, to calculate the extent of burning on deep peat soils and to assess whether there have been changes in burn area over the period 1985–2022. We are aware of no quantitative estimate of the area burnt annually in Scotland over the past few decades. Burning heather moorland has become a highly contentious issue (Davies et al., 2016). Through providing data on the extent and spatial distribution of fires, we hope our study will help inform future debate on this topic.

2 | MATERIALS AND METHODS

2.1 | Study area

We focussed our analysis on Eastern Scotland where the majority of muirburn in Scotland occurs (Douglas et al., 2016). Our study area consists of the Grampian Mountains of North-East Scotland (the Cairngorm Mountains, Monadaliaths, Drumochter Hills, Angus Hills and Breadalbane Hills) and the Southern Uplands in the South-East of Scotland (Lammermuir Hills, Tweedsmuir Hills, Lowther Hills, Moorfoot Hills and Pentland Hills) as shown in Figure 1. These upland areas are largely covered by low-growing moorland vegetation, principally heather with areas of acid grassland and blanket bog (Holden et al., 2007).

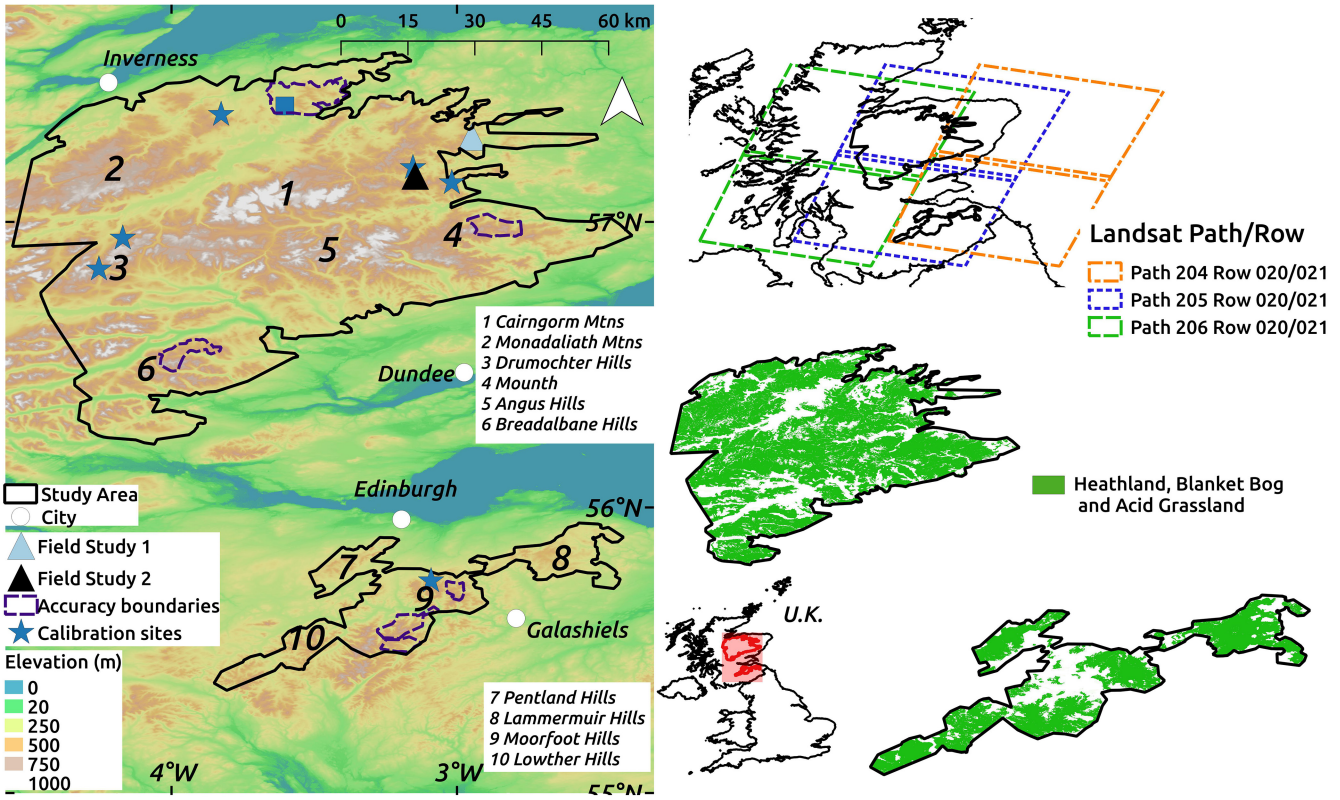

FIGURE 1 Map of study area, showing outline of study areas (black line), location of field study sites (triangles), NBR variability study (square), calibration sites (stars) and accuracy studies (dotted line). Elevation is indicated as shading from dark green (0 m) to white (1000 m).

Mean elevation and slope of the northern study area is 499 m and 10.2°, respectively, compared to 415 m and 10.8°, respectively, for the southern study area (derived from Jarvis et al., 2008). The mountains of the west Highlands provide a rainshadow from the prevailing westerly winds, with annual mean rainfall of 1450 mm/year and 1300 mm/year for the north and south study areas, respectively, with the western sections of both wetter than the eastern (derived from 1991 to 2020 annual precipitation data from Hollis et al., 2019). For the northern study area, summer and winter temperatures are 11.4°C and 1°C, respectively; for the southern study area, 12.3°C and 2.1°C, respectively (derived from 1991 to 2020 seasonal mean temperature data from Hollis et al., 2019). Overall, the study areas have a more continental-style climate (drier, and with cooler winters and warmer summers) compared with the Western Highlands.

We used the 20-m resolution Habitat Land Classification Map 2020 (HLCM2020) (https://spatialdata.gov.scot/geonetwork/srv/api/records/88cea3bd-8679-48d8-8ffb-7d2f1182c175) for the extent of the moorland, defined as 'Raised and blanket bogs', 'Temperate shrub heathland', 'Dry Grasslands', 'Valley mires, poor fens and transition mires', 'Bare Land' and 'Seasonally wet and wet Grasslands'. We excluded 'Alpine and subalpine Grasslands' and 'Artic, alpine and subalpine shrub' where muirburning was rare. Eighty-three per cent and sixty-two per cent of the northern and southern study areas, respectively, were either temperate shrub heathland or raised and blanket bog, whilst 14% and 35%, respectively, were acid grassland (derived from HLCM2020).

We excluded isolated areas of moorland (less than 0.1 ha, equivalent to 10 contiguous Landsat pixels), elevations exceeding 800 m where burning is rare, and any areas of clear-felled forest identified through analysis of Landsat RGB images, and their corresponding NBR values, as well as contemporary Google Earth imagery.

These steps resulted in a study area covering 775,380 ha of moorland under 800 m, consisting of a northern study area (Grampian Mountains) of 682,100 ha and a southern study area (Southern Uplands) of 93,275 ha.

2.2 | Data sources

Information on protected areas was downloaded from the SNH Natural Spaces website (https://www.nature.scot/information-hub/naturescot-data-services). These include Sites of Special Scientific Interest (SSSIs), Special Areas of Conservation (SACs) and Special Protection Areas (SPAs). There is considerable spatial overlap between all three designations. Elevation was taken from the 30-m resolution Shuttle Radar Topography Mission (SRTM; Jarvis et al., 2008) and slope derived from this.

Information on peat soils was taken from the Carbon and Peatland Map (2016) produced by the James Hutton Institute. This dataset classes soils into six categories: deep peat of high conservation value (Class 1), deep peat of potentially high conservation value (Class 2), some areas of deep peat (Class 3), predominantly mineral

soil with some peat (Class 4), deep peat soil but without peatland vegetation (Class 5) and mineral soil (Class 0). Deep peat is specified as a surface peat layer greater than 50 cm in depth. We define deep peat as the combination of Class 1, Class 2 and Class 5. There are 377,500 ha of deep peat in our study area, all but 26,730 ha of this located in the northern study area (see Figure S1).

2.3 | Landsat satellite imagery

We downloaded all Landsat 5, 7 and 8 Level-2 surface reflectance images from May 1984 to July 2022 for Path/Rows 205/020, 204/020, 206/020, 205/021 and 204/021 (see Figure 1) with cloud cover less than 70% from https://earthexplorer.usgs.gov (U.S. Geological Survey, n.d.). In total, this meant 1014 Landsat 5, 632 Landsat 7 and 401 Landsat 8 images. Where available, we used cloud-free imagery from the start of June to the end of September, as these dates lay outwith the muirburning season, and have minimal snow cover. Due to poor coverage from persistent cloud cover, for 10 years (1984–86, 1994, 1997–98, 2007, 2010, 2012 and 2016) we used images from the beginning to mid-October. Later than this date, noise from shadowing on the northern slopes becomes too high for images to be of use.

Many of the Landsat 5 images, especially those from the 1990s, were significantly misaligned, in some cases by as much as 10–20 km. 1 May 1994 (Path/Row 205/020) is an example of such a misaligned image. We used six of these misaligned images, correctly realigning them through a network of locations over Scotland whose positions (latitude and longitude) are precisely known (ground control points). For each misaligned image, we used at least seven ground control points to ensure accurate realignment, with the points that were actually used dependent on cloud cover.

We excluded cloud and cloud shadow using the supplied quality assessment ('QA_Pixel') layer. For each pixel in the image, this layer indicates conditions such as cloud and cloud shadow, allowing these pixels to be masked. This layer sometimes misses clouds, and so the RGB bands of each utilised image were visually examined, and any missed clouds, or cloud shadows, manually masked. The 'QA_Pixel' layer also indicates snow cover. However, many snow banks were missed in this layer, and 'good', non-snow-covered pixels wrongly classified as snow. We therefore manually masked snow-covered pixels from any images that were used.

For each year from 1984 to 2022, the image with the best coverage (least cloud and snow cover) of our study area was chosen as the initial image. For 2018 and 2019, a single image for an area was sufficient. However, for all other years the initial image had at least some masked pixels due to the presence of cloud, cloud shadow or snow. Where available, these masked pixels were replaced with clear pixels from other images from the same year, resulting in a composite image combining imagery from the same year. Over our study area, typically less than 25% of pixels are obscured by cloud or snow (Figure S3) and most pixels have cloud-free data for at least 30 years of our 39-year time series (Figure S2).

This process results in 39 (largely composite) images, one for each year from 1984 to 2022 inclusive. For each of these images, we compute the Normalised Burn Ratio (NBR), as follows:

$$\mathrm{NBR} = \frac{\mathrm{NIR} - \mathrm{SWIR}}{\mathrm{NIR} + \mathrm{SWIR}} \quad (1)$$

For Landsat 5 and 7, the NIR and SWIR bands used are 4 and 7, respectively, whilst for Landsat-8 Bands 5 and 7 were used (see Table 1). NBR is a standard index used for classifying burnt land (de Bem et al., 2020; Gaveau et al., 2021; Santana et al., 2018).

Differences in $\mathrm{NBR}_{\mathrm{unadjusted}}$ may be caused by seasonal variation, atmospheric conditions or use of different Landsat sensors. We investigate the differences these factors cause in Section 2.4.2. To account for the effect these factors may have, a normalisation value (Miller & Thode, 2007; Parks et al., 2014) is added to the $\mathrm{NBR}_{\mathrm{unadjusted}}$ values:

$$\mathrm{NBR}_{\mathrm{adjusted}} = \mathrm{NBR}_{\mathrm{unadjusted}} + \mathrm{NBR}_{\mathrm{offset}} \quad (2)$$

The $\mathrm{NBR}_{\mathrm{offset}}$ is calculated from the mean value of $\mathrm{NBR}_{\mathrm{unadjusted}}$ in a homogenous, unburnt area of moorland in the study region.

From these $\mathrm{NBR}_{\mathrm{adjusted}}$ images, we compute the annual change in $\mathrm{NBR}_{\mathrm{adjusted}}$ (ΔNBR) for each pixel and for a year t as:

$$\Delta\mathrm{NBR} = \left(\mathrm{NBR}_{\mathrm{adjusted}}\right)_t - \left(\mathrm{NBR}_{\mathrm{adjusted}}\right)_{t-1} \quad (3)$$

For the earlier year, any 'NoData' pixels due to snow and cloud contamination were replaced with the NBR value of the previous year. This resulted in 38 ΔNBR images, covering 1985 to 2022 inclusive.

We defined a pixel as burnt if (1) ΔNBR was less than or equal to −0.04, and (2) $(\mathrm{NBR}_{\mathrm{adjusted}})_t$ was less than or equal to 0.2. For the six Google earth calibration sites detailed below in Section 2.4.1,

TABLE 1 Bands of the Landsat satellites used in this study. All these bands have resolution of 30 m.

Landsat 5/7		Landsat 8	
Bands	**Wavelength (μm)**	**Bands**	**Wavelength (μm)**
1 Blue	0.45–0.52	2 Blue	0.45–0.51
2 Green	0.52–0.6	3 Green	0.53–0.59
3 Red	0.63–0.69	4 Red	0.64–0.67
4 Near-Infrared (NIR)	0.77–0.9	5 Near-Infrared (NIR)	0.85–0.88
7 Infrared (SWIR)	2.08–2.35	7 Infrared (SWIR)	2.11–2.29

the false positive rate and true positive rate were plotted for a few ΔNBR classification thresholds, resulting in a graph known as a receiver operating characteristic (ROC) curve (Hoo et al., 2017). The value closest to the top left-hand corner was selected as our threshold value (see Figure S4a). We define the burning season as October to April inclusive (e.g. 2019 includes fires from October 2018 to April 2019).

Many fires are smaller than an individual Landsat pixel. We used data from Google Earth imagery (Section 2.4.1) to estimate the fractional area of each Landsat pixel burnt. We developed a simple linear relationship linking ΔNBR and burnt area (Section 3.1.1).

The Mann–Kendall test and the Theil–Sen estimator were applied to quantify trend significance and trend magnitude, respectively, in the time series of annual burnt area for the two separate study areas. Mann–Kendall is a rank-based nonparametric test of whether a monotonic trend exists in a time series, whilst the Theil–Sen estimator is a nonparametric technique for estimating the magnitude of a linear trend, which is insensitive to outliers. All the image processing and statistical tests were done in Python2.7 using the 'rasterio' and 'gdal' packages.

2.4 | Calibration studies

2.4.1 | Use of Google Earth to calibrate results

Muirburns are frequently of a similar size to an individual Landsat pixel (0.09 ha) which, combined with the shape of many burns (rectangular, long and thin), means the fractional burned area of any one pixel is often less than 50%. Assuming each Landsat pixel classified as burnt is 100% burnt can therefore lead to an overestimate of burnt area. To investigate this issue, we use six sites covering 910 ha, two each covered by Google Earth imagery from 2021, 2020 and 2019. Five sites are in the northern study area and one in the southern (see 'Calibration Sites' in Figure 1). In each area, we used this Google Earth imagery to delineate the outline of burns for that year's imagery. We then used Huber regression to obtain a relationship between the ΔNBR of a pixel obtained from the Landsat imagery and the fractional area of pixel burnt indicated by the Google imagery. Site was used as an additional covariate. Huber regression is a linear regression model that is robust to outliers, effectively scaling down the outlier's contribution though not completely ignoring their effects. Because means are not robust, to estimate the goodness-of-fit of the relationship, an adjusted goodness-of-fit metric that used the median of the observed data instead of the mean was utilised (Leroy & Rousseeuw, 1987) where y are the observed values of area burnt and f are the burnt areas estimated by the model.

$$R^2 = 1 - \frac{\text{median}\left(y_i - f_i\right)^2}{\text{median}\left(y_i - y_{\text{median}}\right)^2} \quad (4)$$

The six accuracy assessment and two field study sites (see Figure 1) were used to assess the accuracy of this fractional classification approach for a number of ΔNBR thresholds. In comparison, we also calculated accuracy for the case where any pixel that satisfied the conditions for ΔNBR and $(\text{NBR}_{\text{adjusted}})_t$ was classified as fully burnt. We refer to this latter case as binary classification as the pixel is classified as either completely burnt or completely unburnt. The accuracy was assessed using the true positive rate (TPR) and the false positive rate (FPR). The TPR and FPR are calculated, respectively, as

$$\text{TPR} = \frac{\text{Landsat Burn that is Burn}}{\text{Landsat Burn that is Burn} + \text{Landsat No Burn that is Burn}} \quad (5)$$

$$\text{FPR} = \frac{\text{Landsat Burn that is No Burn}}{\text{Landsat Burn that is No Burn} + \text{Landsat No Burn that is No Burn}} \quad (6)$$

2.4.2 | Variation in NBR—Time series

Whilst ideally we would have used imagery from approximately the same date every year, the study area's cloudiness meant this was not feasible. Additionally, both Landsat 5/7 (ETM) and Landsat 8 (OLI) sensors were used. It has been suggested that, dependent on land use, differing NBR values are obtained from these different sensors (Mancino et al., 2020). Therefore, to examine the variability of NBR in moorland over the seasons, the effect of burning on NBR, and whether NBR values differed between the sensors used in Landsat 5/7 and Landsat 8, we carried out two time-series studies. The first computed mean NBR from 2013 to 2020 for 10 moorland patches in the North-East of Scotland that were burnt in winter 2017 (see 'NBR Variability Study' in Figure 1).

The second examined mean NBR over the whole study period for two unburnt areas of moorland, one in the Grampian Mountains and the other in the Southern Uplands, covering 22,770 and 3585 ha, respectively. In 1954, the Cairngorms National Nature Reserve was created, with a stated objective of keeping human intervention to a minimum, and as a result, in this area muirburning was largely eschewed. Even after the reserve was abolished in 2006, this voluntary moratorium was largely adhered to, and burning is minimal. This area is therefore ideal to check the susceptibility of NBR values to seasonal and sensor effects. An area in the Southern Uplands which had a low burning rate was also chosen. Within these two selected areas, we found no sign of burning in the Landsat imagery over the studied time period. The mean $\text{NBR}_{\text{unadjusted}}$ value for each site was computed for the available imagery.

2.5 | Validation study

2.5.1 | Field study

Two field study sites were chosen, both in the eastern Grampian Mountains (see Figure 1). All fieldwork was done in August 2021, to accord with the Landsat images of the area used to determine burning (Landsat 7 from 9 August 2020 and a Landsat-8 image

from 17 August 2021). The first site (Ladder Hills) was the southern and northern slopes of an eastwards descending ridge. The vegetation was dominated by *C. vulgaris*. Areas of the south-facing slope had been burnt in the 2020–2021 burning season, with other areas burnt in prior years. Elevation ranged from 400 to 600 m and slopes from about 15° at the northern and southern foot of the ridge, progressively declining to about 5° towards the top of the ridge.

The second site (Strathdon Hills) consisted of the eastern and western facing slopes of a northward descending ridge. It was also dominated by *C. vulgaris* along with reindeer lichen (*Cladonia portentosa* (Dufour) Coem.) and crowberry (*Empetrum nigrum* L.). Areas of both slopes had been burnt in the 2020–2021 burning season. Elevation ranged from 450 to 550 m, with slopes of 5° to 15°.

The HLCM 2020 raster classed both areas as 'Temperate shrub heathland', with smaller areas of 'Raised and Blanket Bog'. For both sites, the entire study area was walked, and the perimeter of patches burnt in the 2021 season recorded using GPS (Garmin GPSMAP64s).

2.5.2 | Use of Google Earth and Sentinel-2 to estimate accuracy

To produce an estimate of the error rate, we used recent Google Earth imagery (https://www.google.com/earth/index.html) alongside European Space Agency (ESA) Sentinel-2 imagery. We chose six sites across our study area, with three each situated in the northern and southern study areas. Each site was covered by a different year of Google Earth imagery—2013, 2016, 2017, 2019, 2020 and 2021—and in total covered an area of 41,147 ha (see 'Accuracy Boundaries' in Figure 1). Within these sites, the boundaries of all muirburns seen in the high-resolution Google Earth imagery were delineated. Google Earth imagery has been used in previous studies to estimate muirburn distribution (Douglas et al., 2016; Matthews et al., 2020). To determine whether the burn was carried out in that year's burning season, the S-2 imagery (10-m resolution RGB images) from the previous year was examined, where the absence of the burn on the S-2 image, and its subsequent appearance on the Google Earth imagery, could be readily seen. Recent muirburns look different from older burns, and so for the 2013 year, when no Sentinel imagery was available, we used this quality to judge whether a muirburn had been carried out in that year.

The resultant area burnt was then calculated across the sites and compared with the area given by our ΔNBR Landsat time-series raster for that year. Furthermore, the Landsat time-series area classified as burnt that corresponded to the Google Earth burn (true positive (TP)), the Landsat area classified as burnt that was unburnt in the Google imagery (false positive (FP)) and area that was burnt that was classified as unburnt in Landsat (false negative (FN)) were all calculated and recorded in a confusion matrix, with the producer's and user's accuracy given. Producer's accuracy is the burnt area that Landsat correctly classified divided by the Google Earth burnt area, and so equivalent to the true positive rate (Equation 4) expressed as a percentage:

$$\text{Producer's accuracy} = \frac{\text{TP}}{\text{TP} + \text{FN}} \times 100 \tag{7}$$

$$\text{Producer's accuracy} = \text{TPR} \times 100 \tag{8}$$

User's accuracy is the burnt area that Landsat correctly classified divided by the area that Landsat classified as burnt.

$$\text{User's accuracy} = \frac{\text{TP}}{\text{TP} + \text{FP}} \times 100 \tag{9}$$

$$\text{User's accuracy} = \frac{\text{Landsat Burn that is Burn}}{\text{Landsat Burn that is Burn} + \text{Landsat Burn that is No Burn}} \times 100 \tag{10}$$

Estimated error ranges for the total annual burn areas were computed using Monte Carlo simulations (a thousand runs) from the false positive and false negative error rates extracted from the validity study confusion matrices. Monte Carlo simulation is a powerful technique for incorporating uncertainty into models by repeatedly sampling from probability distributions.

2.6 | Effect of muirburn on air quality

Muirburning can degrade local and regional air quality with negative impacts on human health. We estimate the particulate matter (PM) emissions from muirburn assuming only combustion of above-ground vegetation (i.e. no combustion of peat) using:

$$E = A.B.F.E_F \tag{11}$$

where A is area burnt (in units of ha year^{-1}), B is biomass loading (assumed as 1300 g m^{-2}), F is fraction burnt (assumed as 0.9), and E_F is emission factor (assumed as 15 g kg^{-1}). Values for B, F and E_F are default values for grasslands from (Wiedinmyer et al., 2011). Fuel loads of 500–2000 g m^{-2} have been reported for Scottish moorlands (Davies et al., 2008), matching the default values we assumed.

3 | RESULTS

3.1 | Calibration studies

3.1.1 | Calibration using Google Earth imagery

Figure 2 shows ΔNBR from the Landsat imagery against the fractional area of pixel burnt indicated from the Google Earth imagery. Huber regression gives us the following relationship between ΔNBR and area burnt (in m^2, maximum 900 m^2) for each pixel:

$$\text{Area burnt}\ (\text{m}^2) = [(\Delta\text{NBR} \times\ -660) + 1] \times 9 \tag{12}$$

We report area burnt based on this equation. The 97.5% confidence intervals for the gradient are −638.5 to −680 and for the intercept −0.8 to 2.

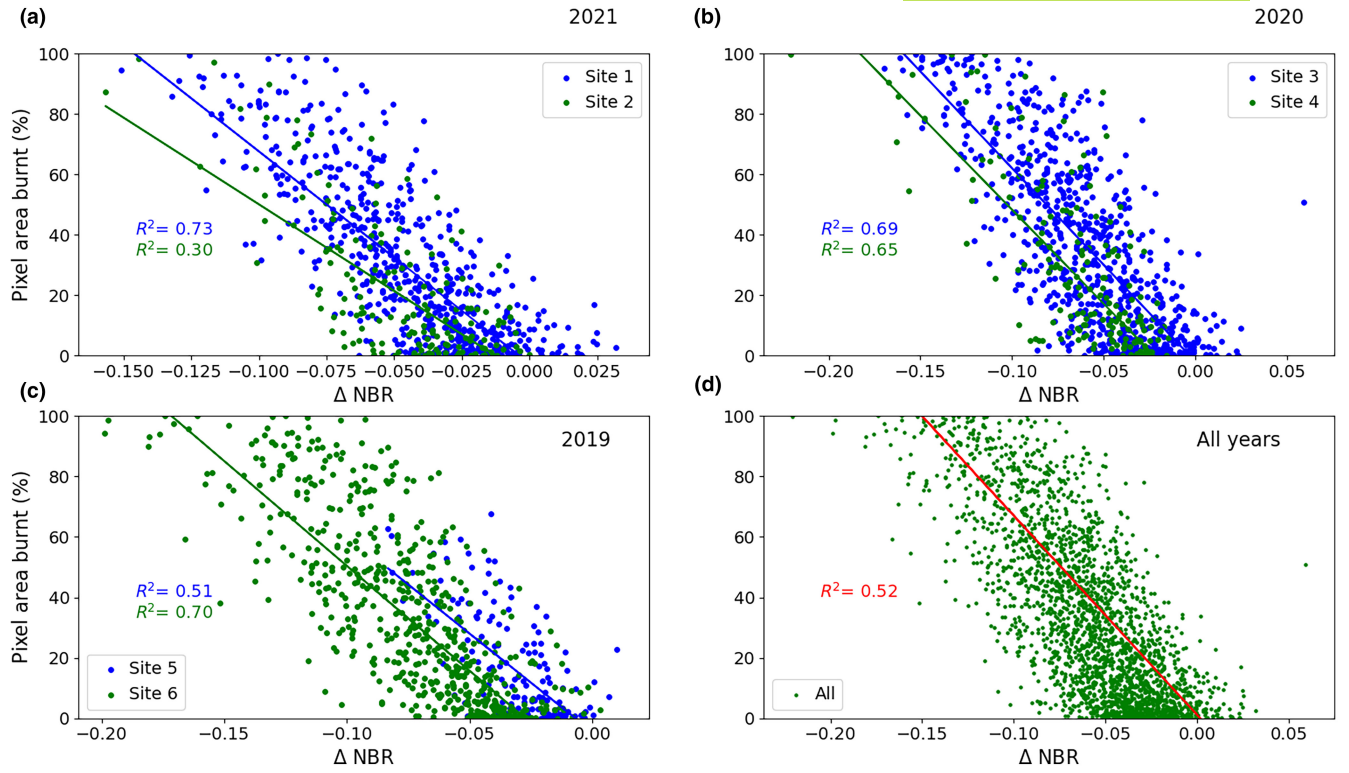

FIGURE 2 Fractional area of a pixel burned (%) versus ΔNBR for that pixel for six calibration sites, two each in (a) 2021, (b) 2020, (c) 2019 and (d) all years together.

3.1.2 | NBR variability study

Figure 3 shows the variability in NBR between 2011 and 2021 across 10 different moorland areas that were burnt in 2016–2017. We note an increase in moorland NBR from spring values (April and May) to summer and autumn, possibly coinciding with the commencing of the growing season. The variability in the $NBR_{unadjusted}$ (Figure 3a) of unburned moorland shows the requirement for the NBR_{offset} term (Figure 3b). Burning causes a sharp reduction in NBR.

Figure 4 shows the variation in mean $NBR_{unadjusted}$ by Landsat sensor and time of year for relatively homogenous, unburnt moorland. NBR is lowest in April and May, and peaks in July and August, and is consistently above the NBR values of burnt areas (Figure 3).

3.2 | Validation study

3.2.1 | Estimation of error—From Google Earth, S-2 imagery and field studies

In our two field studies, we recorded 182 and 137 burns, covering 10.7 and 17.6 ha, at field Study Sites 1 and 2, respectively. The outline of the burns laid over the Landsat NBR and ΔNBR pixels can be seen in Figure 5. The largest burn was 0.57 ha (at Site 2) and the smallest 26 m^2 (at Site 1). Mean (median) burn size was 0.06 ha (0.04 ha) and 0.13 ha (0.09 ha) at Sites 1 and 2, respectively.

Using Google Earth, over the six accuracy assessment and two field study sites covering 41,600 ha, we found 3900 ha of burnt land caused by 6073 burns, with a mean size of 0.6 ha (see Table 2). We give the confusion matrix for Site 1 for 2021 in Table 3, whilst the other site's confusion matrices are found in Tables S1–S15.

Our Landsat time-series estimate gave a total burnt area of 3330 ha, an underestimate of 15% of the real burnt area of 3893 ha. We report 328.8 ha of this Landsat estimate was false positives, not containing any burn area. The main sources of this error are pixels along both watercourses and tracks and areas of shadow on steep north-facing slopes and gullies. The boundary between clear-felled forest and our study area contributed false positives when the study area edge pixels partially overlay the plantation. Other disturbances (scrapes, quarry activity, track construction and landslips) caused false positives, but contributed less than 10 ha in total, equivalent to about 0.2% of burn area. Overall producer's accuracy for burns is 77%, and user's accuracy is 90.1%. Of the 6073 burns, we correctly identified at least one burnt pixel for 4380 (72%) burns. Site 3 was notably much poorer in this respect than the other sites, with only 1003 (54%) of the 1859 burns identified.

Site 5 was unusual, with a high number of false positives and consequently a very low user's accuracy (see Table S10). This site, in the South-West of the Southern Uplands, was atypical, largely consisting of acid grassland, interspersed with smaller heather patches, whereas most of our study area is heather, with small patches of acid grassland. Burning was infrequent on this site, and false positives seemed higher on grassland areas than on heather. The low

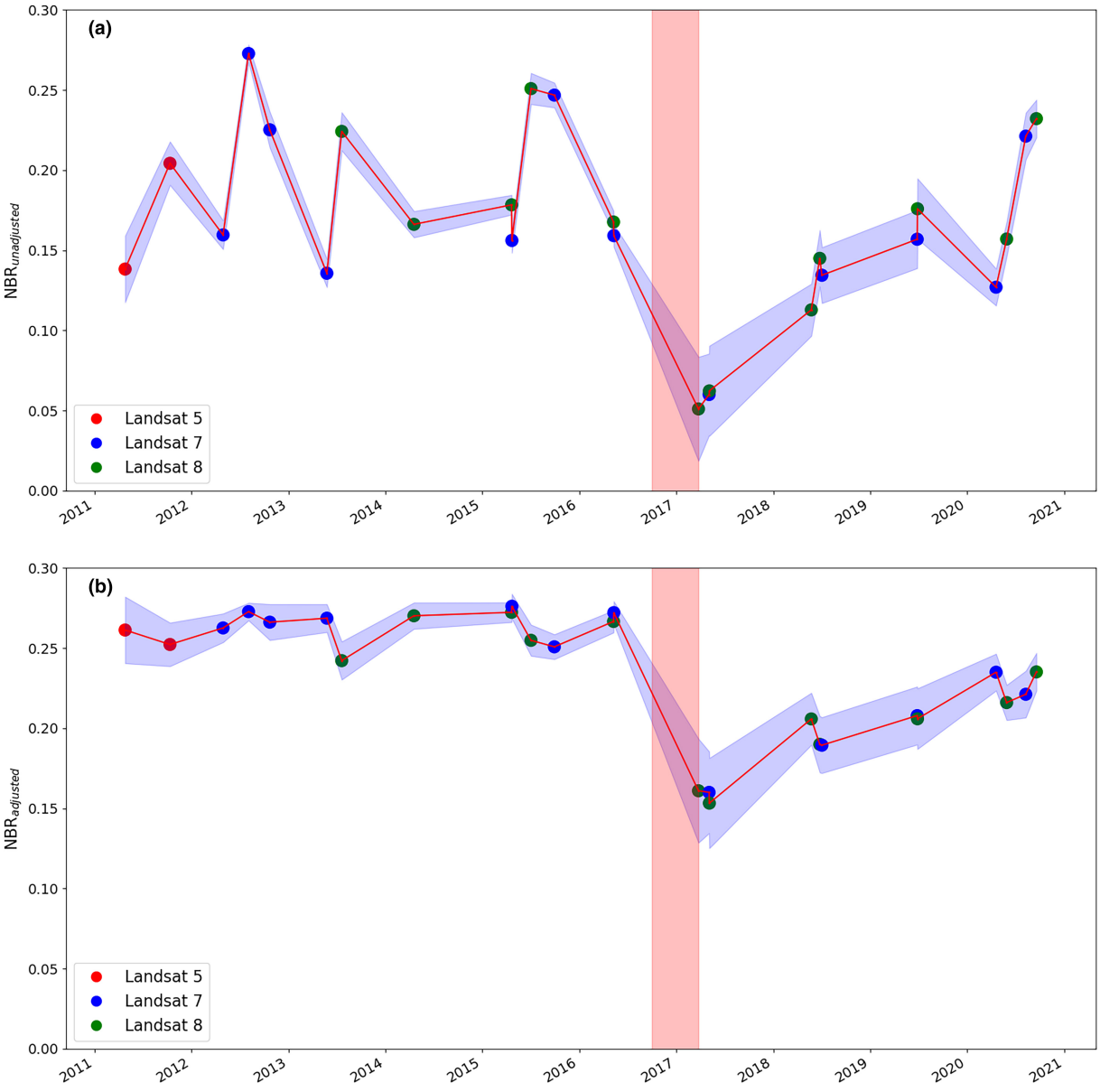

FIGURE 3 Variability in (a) mean $NBR_{unadjusted}$ and (b) mean $NBR_{adjusted}$ calculated over 10 moorland areas burnt in 2016–2017. Blue shading shows 95% confidence intervals calculated from the pooled standard deviation of the pixels in the 10 areas. The shaded red vertical column shows time period in which the areas were burnt.

producer's accuracy for Site 3 (see Tables S6–S8) was probably attributable to the small size of burns on this site.

3.2.2 | Comparison of fractional and binary Landsat pixel classification

Equation (12) was used to calculate the fractional area of a Landsat pixel burnt. Figure S4 shows the accuracy of this approach (fractional classification) compared with the use of binary classification, with the TPR and FPR values shown for a number of ΔNBR thresholds. It can be seen that fractional classification consistently yields more accurate results than binary classification.

3.3 | Burnt area

3.3.1 | Grampian Mountains

During 1985–2022, estimated area burnt across the Grampian Mountains was 4670 ± 290 ha (mean ± standard error; Figure 6a). Substantial annual variability is likely due to real year-to-year variability in fire combined with year-to-year differences in cloud occurrence impacting the detection of burns. Burning was concentrated along the eastern portion—to the east of Ben Chonzie, Ben Vrackie, Braemar and Grantown on Spey, and to the north, west and north-west of Grantown on Spey (Figure 7a, Figure S5).

There was no significant annual increase in estimated area burnt from 1985 to 2022 ($z = 1.7$, $p = 0.09$, Mann–Kendall test; estimated

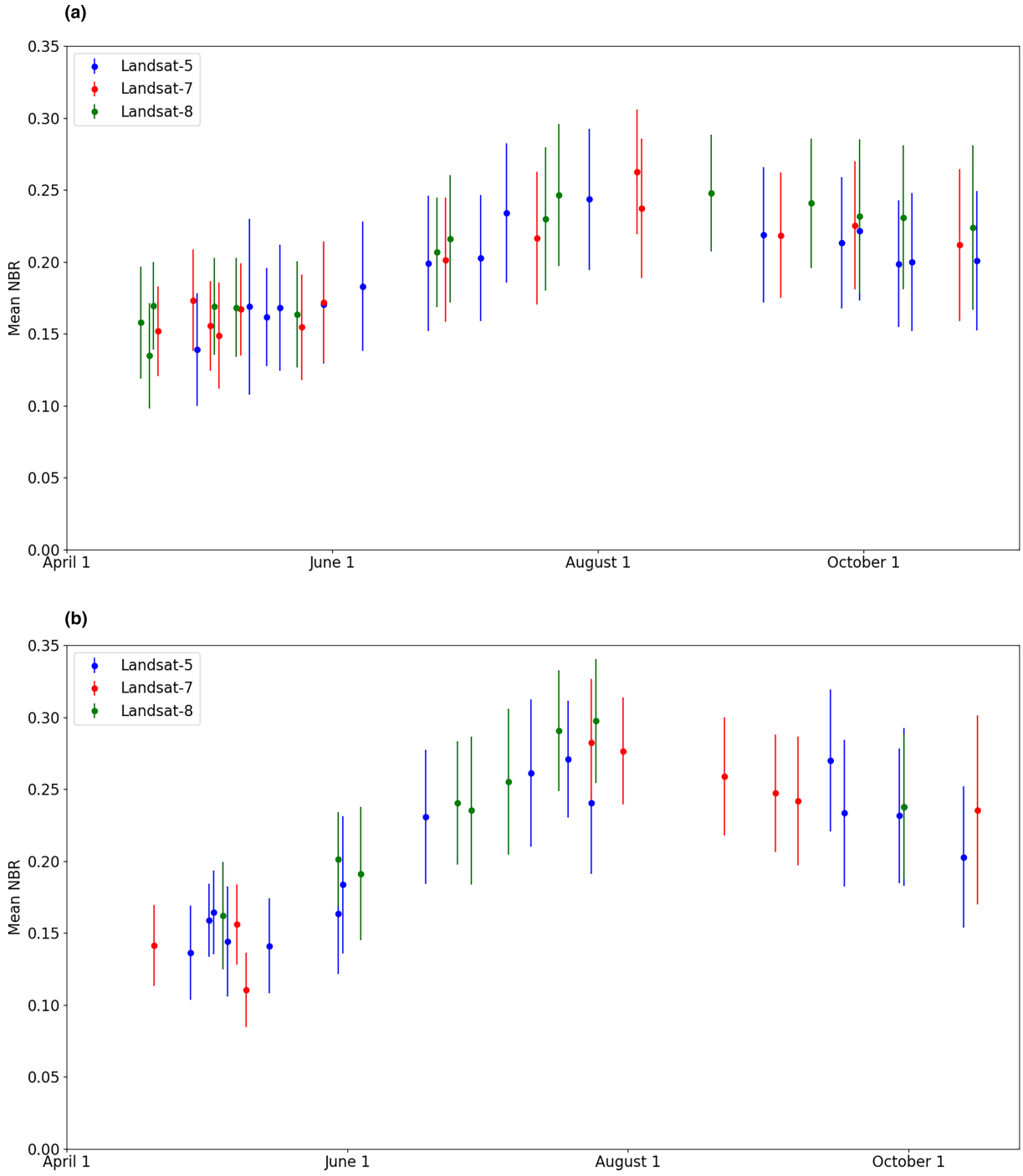

FIGURE 4 Variability in mean $NBR_{unadjusted}$ across relatively homogenous, unburnt moorland for (a) northern study area and (b) southern study area. Error bars show standard deviation.

increase of 46 ha year^{-1}, 95% confidence intervals between −12 and 99 ha year^{-1}). The lack of significance is more marked if we exclude 1985 and 1986 (low area burnt in these years largely caused by cloudy conditions from 1984 to 1986 giving $z = 0.9$ and $p = 0.4$).

Total burn area was dominated by small burns. Burns over 1 ha in size (consisting of at least 11 *fully burnt* contiguous pixels) accounted for 17% of burn area, varying from a minimum of 5% in 2020 to a maximum of 36% in 2019. Burns over 5 ha accounted for 8% of burn area, ranging from 1% in 2021 to 31% in 2019.

Mean elevation of burns was 443 m and mean slope 10° (see Figure 8a). Three per cent of burnt area was on slopes above that of the Muirburn Code's recommended limit of 27°, though this may be an overestimate as in our accuracy study 'noise' (false positives) were preferentially found on steeper north-facing slopes in shadow.

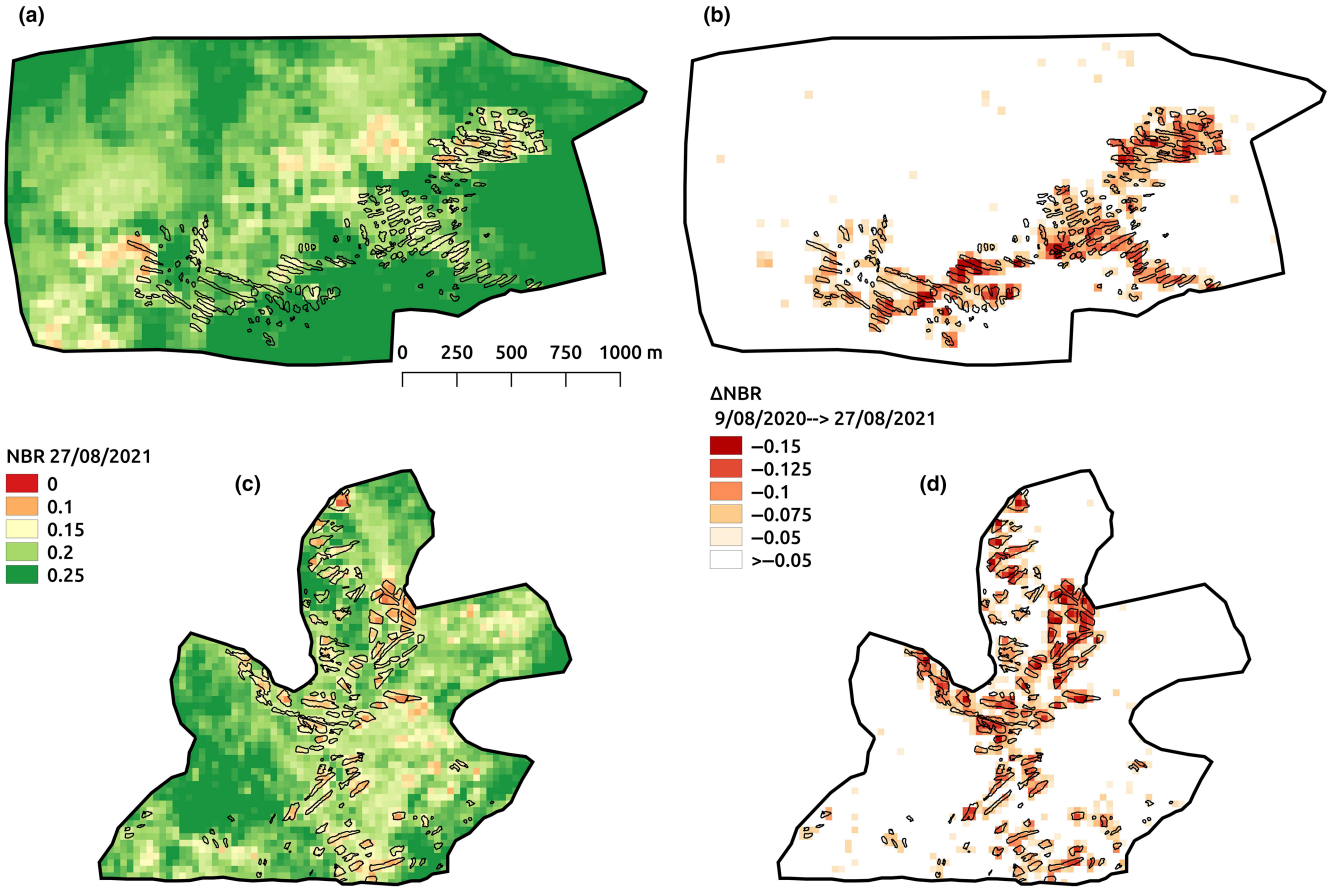

FIGURE 5 Field survey showing prescribed burns (outlines in black) plotted over Landsat imagery. (a, c) NBR calculated from Landsat-8 (27 August 2021 image). (b, d) ΔNBR between 9 August 2020 and 27 August 2021. Study site 1 shown in (a, b); Study Site 2 shown in (c, d).

3.3.2 | Southern Uplands

Estimated burnt area was concentrated in the Lammermuir Hills in the east of the Southern Uplands (Figure 7b, Figure S6). The mean ± standard error burnt area was 1410 ± 120 ha (Figure 6b). The increase in burning over the study period was not statistically significant ($z = 1.7$, $p = 0.08$; estimated increase of 19 ha year^{-1}, with 95% confidence intervals of between −4 and 43 ha year^{-1}), particularly if 1985 is excluded ($z = 1.2$, $p = 0.2$). The lowest value of burnt area (in 2012) was due to poor coverage and possibly the construction of wind farms in the Lammermuir Hills region reducing the quantity of burning carried out, though burning resumed here in the subsequent years. Mean elevation of burns was 398 m and mean slope 9.2°, with 2% of burnt area above 27° (Figure 8b). Large burns (>1 ha) made up 21% of burn area, varying from a low of 5% in 1989 and a high of 38% in 2000. Very large burns (>5 ha) comprised an average of 8% of total burn area.

3.4 | Burning on peat and in protected areas

Figure 6 also shows the estimated area of burning that occurred on deep peat (classified as Categories 1, 2 and 5 collectively). In the Grampian Mountains, 34% (1590 ha year^{-1}) of burning occurred on deep peat, compared to 23.4% (330 ha year^{-1}) of burning in the Southern Uplands. Deep peat accounted for 50% and 24% of the moorland in the Grampian Mountains and Southern Uplands, respectively. There was no significant change in burn area on deep peat over the study period. Following the introduction of the revised Muirburn Code in 2017, which recommended against burning on peatlands, no decline was found in the peat area burnt, with an average of 31.4% (1865 ha year^{-1}) of burning on peat from 1985 to 2017 and 32% (2280 ha year^{-1}) from 2018 to 2022.

In the northern study area, moorland covered by 35 SAC, 18 SPA and 90 SSSI designations totalled 77,940, 203,820 and 107,680 ha, respectively, with considerable spatial overlap between the three categories. On average, 0.7% of the northern study area was burnt annually, compared with a mean of 0.5% of SAC, SPA and SSSI area. A large fraction (e.g. about 40% of SAC area) of protected area consisted of the Cairngorms, which had a low rate of burning of about 0.4%. Outwith the Cairngorms, burning in protected areas was about 0.7%.

In the southern study area, moorland covered by 5 SAC, 28 SSSI and 3 SPA designations totalled 8890, 590 and 19,145 ha, respectively. On average, 1.5% of the southern study area was burnt, whilst a mean of 1%, 5% and 1.4% of SACs, SPAs and SSSIs was burnt annually, respectively.

TABLE 2 Details of accuracy assessment sites. Latitude and longitude give coordinates of site's centroid. Year indicates burning season. Users and prod. indicate the user's and producer's accuracy for burnt areas, respectively. Burn no. is number of burns. FS1 and 2 indicate respective field study sites.

Site	Latitude	Longitude	Year	Area (ha)	Burn no.	Burn area (ha)	Users (%)	Prod. (%)
1a	57.437855	−3.534627	2021	15,935	659	503.9	96.2	57.9
1b	—	—	2020	—	129	85.7	77.1	60.2
1c	—	—	2019	—	428	2086.7	99.8	82.1
2a	56.983815	−2.86676	2019	6642	300	148.8	97.5	92.4
2b	—	—	2018	—	216	139.6	96.7	84.4
2c	—	—	2017	—	288	128.1	40.5	75.8
3a	56.540875	−3.954349	2018	6712	35	3.9	59.6	31.7
3b	—	—	2017	—	973	115.2	86.5	36.7
3c	—	—	2016	—	851	147.9	85.7	67.7
4	55.588468	−3.185695	2013	6295	49	84.9	91.0	70.1
5	55.519358	−3.197667	2016	3427	29	17.1	27.8	58.3
6a	55.710726	−3.005332	2021	2126	843	187.4	68.5	93.7
6b	—	—	2020	—	456	147.7	92.0	89.4
6c	—	—	2019	—	498	67.7	98.9	73.2
FS1	57.297693	−2.947927	2021	243	182	10.7	100	40.0
FS2	57.160348	−3.147791	2021	221	137	17.6	99.4	92.7
All	—	—	—	41,601	6073	3893	90.1	77.1

TABLE 3 Confusion matrix comparing burnt area obtained from Google Earth and from Landsat time series over 16,000 ha of moorland in North-East Scotland (Site 1) for the year 2021.

Google Earth (reference data)				
Landsat		No burn (ha)	Burn (ha)	Total (ha)
	No burn	15419.7	212.2	15631.9
	Burn	11.5	291.7	303.2
	Total	15431.2	503.9	15,935

3.5 | Impact of muirburning on air quality

With the assumptions given in Section 2.6, and using an annual area burnt of 6100 ha year^{-1}, we estimate muirburn releases 1000 tonnes of PM annually. This is equivalent to transport emissions from Scotland (Transport Scotland, 2018), suggesting a potential contribution of prescribed burning to regional air quality degradation.

4 | DISCUSSION

We present the first analysis of annual muirburn across Scotland using Landsat imagery. The 30-m spatial resolution of Landsat imagery allows relatively small and fragmented burn areas to be mapped. Our field study indicated an average burn size of 0.1 ha, compared with a Landsat pixel size of 0.09 ha. The 16-day repeat cycle and extensive cloud cover preclude mapping of burnt area at higher temporal resolution than annual time series provided here. We used two methods to analyse the effectiveness of our approach. First, we conducted a field study in two areas in which burnt area was carefully mapped and compared with our Landsat results. Second, Landsat burnt area was compared with burn area obtained from the higher resolution Google Earth imagery. Both approaches corroborate our approach and provide evidence that our numbers are robust.

There have been few studies mapping the extent of muirburn in Scotland. A UK-wide visual analysis of aerial photography and Google Earth imagery (Douglas et al., 2016) produced a burn map (their Figure 1a), which shows a very similar spatial distribution of burns to our analysis. A study in the English uplands assessed aerial photography for a random sample of 2% of the study area (10,360 km^2) and estimated an annual burn area of 11,400 ha year^{-1} in the year 2000 (Yallop et al., 2006). Our estimated rate of burning in the Scottish uplands is 0.8% year^{-1} (or about 0.95% year^{-1} if we apply the 15% underestimate in burn area suggested by Section 3.2.1), which is similar to the 1.1% year^{-1} rate of burning in the English uplands (Yallop et al., 2006). Hester and Sydes (1992) used aerial photography from 1988 of 32 randomly chosen sites in the Grampian Mountains and Southern Uplands, which suggested an annual burn rate of between 1% and 2%, the lower bounds of which is similar to our estimates.

Estimated annual burnt areas varied from 4000 to 8000 ha in the Grampian Mountains and 1000 to 3000 ha in the Southern Uplands. This interannual variability in area burnt is likely due to real variability in burning and to variability in cloud coverage obscuring images and causing burns to be allocated to the following year. In the

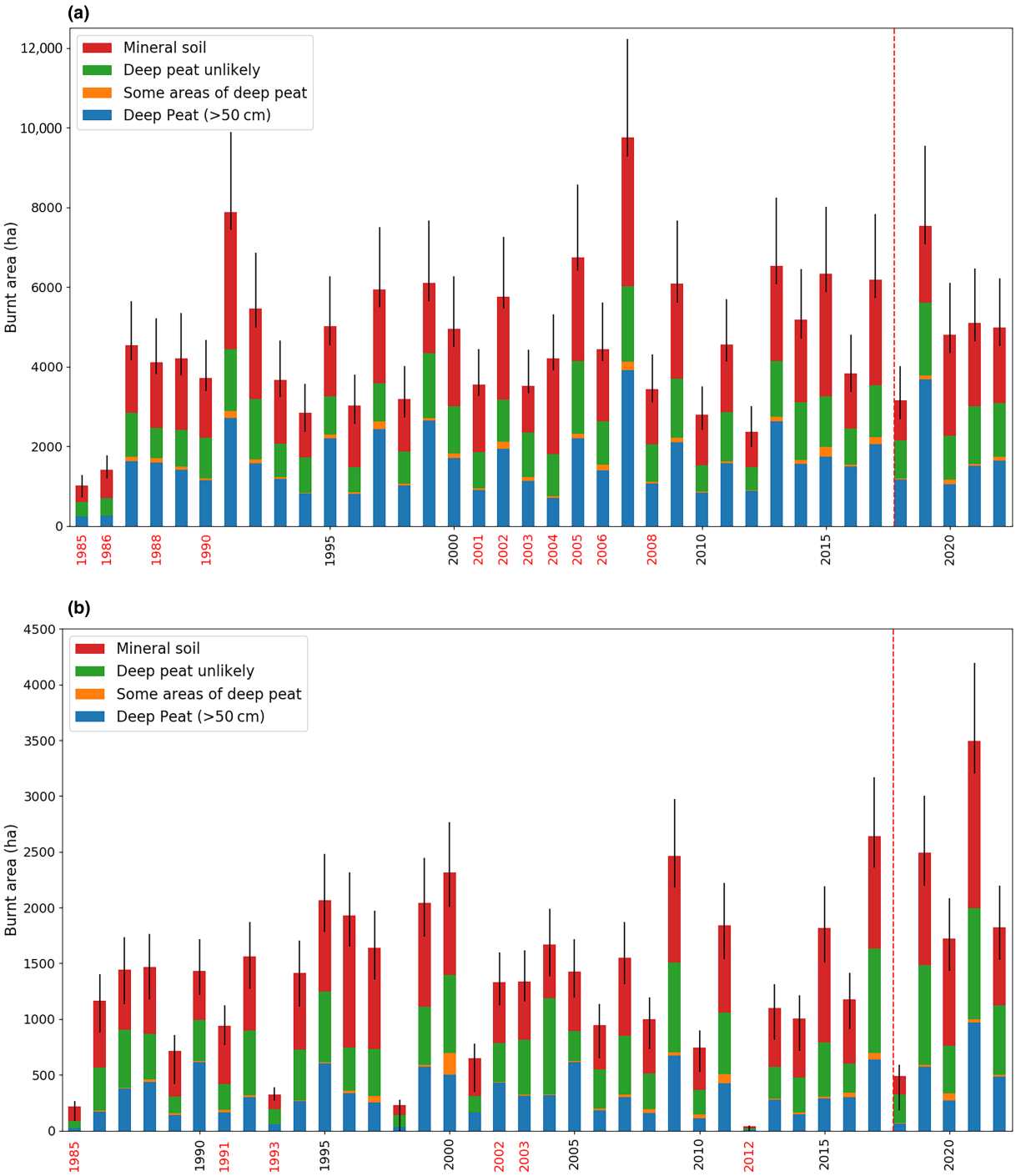

FIGURE 6 Estimated annual area burnt in (a) Grampian Mountains and (b) Southern Uplands during 1985–2022. Stacked bars show area burned by category of underlying soil and peat. Years indicated in red text had less than 75% cloud-free pixel coverage area for their respective study area. Vertical dotted red line shows first year revised Muirburn Code was in effect. Error bars show the estimated uncertainty in total annual area burnt, computed from false positives and false negatives of validity study (see Section 2.5).

Grampian Mountains, estimated area burnt varied from 6200 ha in 2017 to 3150 ha in 2018. Both years had almost completely clear coverage of the study area and so variability is likely to be influenced by weather conditions in the burning season, with especially wet years resulting in a decrease in area burnt, and dry, calm years increasing area burnt. A mild and snow-free winter season is likely to have caused greater burning in 2017.

We found no significant trend in estimated area burnt over the period 1985 to 2022. Douglas et al. (2016) counted the number of fire hot spots throughout the burning season and reported increasing burn frequency from 2001 to 2011 across Scotland. We found no significant increase in estimated burnt area during 2001–2011, although this period corresponded to poor availability of cloud-free images, and we use map burn area rather than hot spots so that our

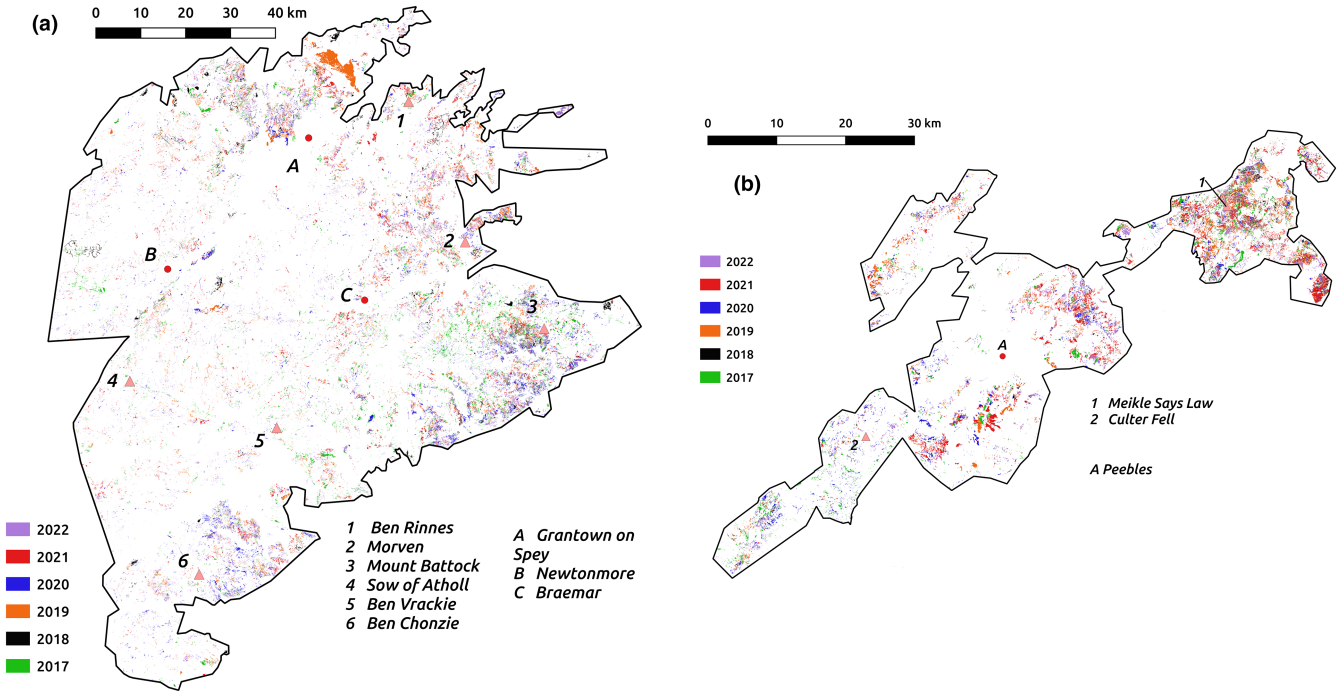

FIGURE 7 Estimated burnt area during 2015 to 2022 (a) Grampian Mountains and (b) Southern Uplands. Selected peaks (triangles with associated numbers) and settlements (dots with associated letters) are shown.

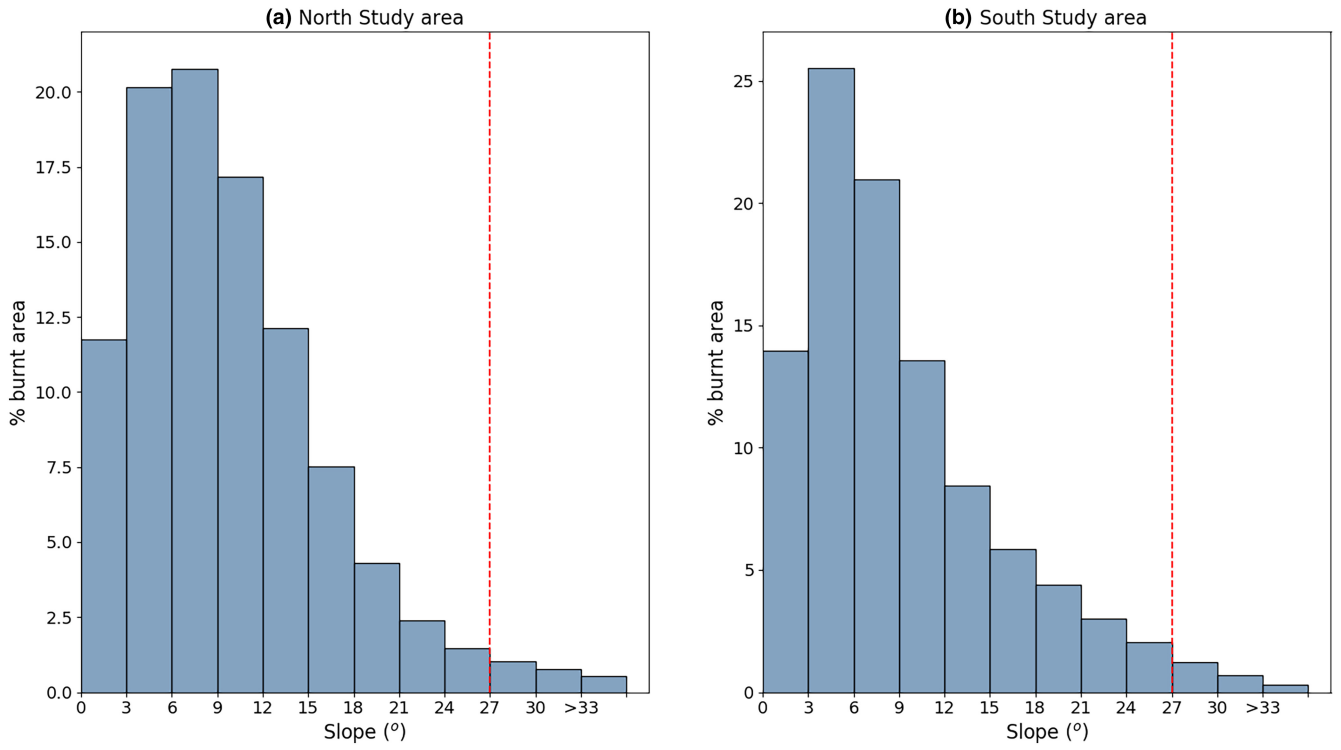

FIGURE 8 Fraction of burn area as a function slope of land (in degrees) for (a) Grampian Mountains and (b) Southern Uplands. Red dotted vertical line shows suggested maximum slope of burnt land.

results are not directly comparable. A study of aerial photography from the mid-1940s, mid-1960s and 1988 (Hester & Sydes, 1992) of 32 sites in the Grampian Mountains and the Southern Uplands found a significant decline in area burnt in the Grampians but no change in the Southern Uplands over their study period. Another study of aerial photos (Hester et al., 1996) taken in 1946–1950 and 1988 over 936 km^2 in North-East Scotland also found a significant decline in muirburning over the time period, with the fraction of heather moors

classified as being burnt declining from 26% to 10%. Our study suggests that any decline in burnt area halted in the 1980s, as from 1985 to 2022 we found no significant change in estimated annual area burnt in either the Grampian Mountains or the Southern Uplands.

To improve our burnt area estimates, we used a derived linear relationship to estimate the proportion of Landsat pixel that was burnt. This meant using subpixel burnt area (fractional classification), as opposed to a binary wholly burnt/unburnt classification, where any pixel below the threshold NBR value is regarded as wholly burnt. For both our six calibration sites, and our six verification areas and the two field study sites, the binary burnt/unburnt classification gave less accurate results than the fractional classification, with higher false positive and lower true positive rates over a range of ΔNBR threshold values (see Figure S4). No significant trends were seen in the burnt area time series regardless of whether we used subpixel estimates of burnt area or wholly burnt pixels.

Our analysis suggests burning on deep peat is widespread, comprising 1920 ha $year^{-1}$ or 31.5% of area burnt. This figure is comparable to a previous estimate of 27.6% based on analysis of aerial photography from 2011 and satellite photography from 2001 to 2010 (Douglas et al., 2016). However, we note that peat depth can vary on scales of just a few metres, and the 'Carbon and Peatland Map' that we used to indicate the location of deep peat may not necessarily capture the fine spatial variation of soil type. The revised NatureScot Muirburn code suggests that burning should not occur on peat unless it is part of a habitat restoration plan approved by NatureScot. We found no significant change in area burnt on deep peat since this revision, suggesting that it has not been widely adopted by land managers. At present there is a government proposal in Scotland to introduce licencing for all muirburning, with a ban on burning on deep peat (deeper than 0.4 m) except for restoration of the natural environment, wildfire prevention or research (ScotGov, 2023). A prohibition on burning on peat over 0.4 m deep within protected moorland areas is already in place in England (UKGov, 2021) though its effectiveness has been disputed. (Greenpeace, 2022; RSPB, 2023).

The widespread burning of areas of deep peat that we document here is likely to have negative impacts on a wide range of environmental services (Worrall et al., 2011). Previous work has shown burning on peatlands reduces carbon sequestration (Garnett et al., 2000; Marrs et al., 2019) and reduces carbon stocks in surface peat (Ward et al., 2007). Burning peatland also increases downstream flood risk (Holden et al., 2014, 2015) and increases erosion (Li et al., 2018) as well as reducing macro-invertebrate diversity (Brown et al., 2013) and stream water quality (Clay et al., 2012; Ramchunder et al., 2013).

Many UK peatlands have been artificially drained (Holden, Chapman & Labadz, 2004; Holden et al., 2007) making them more susceptible to wildfire and increasing the likelihood that prescribed burns will damage the peat. Peatland restoration, which can be achieved by blocking drains, raises the water-table depth and provides a range of environmental benefits (Evans et al., 2021; Parry et al., 2014; Ramchunder et al., 2012; Wallage et al., 2006; Worrall et al., 2007) including a reduction in the risk of fire (Glaves et al., 2020). Warmer and drier conditions due to climate change (Gallego-Sala et al., 2010) can further exacerbate the risk of fire in degraded peatlands and provide greater urgency to restore peatland hydrology.

Our analysis cannot distinguish between wildfire and prescribed fire. Wildfires occur across the study area and are subject to yearly fluctuations, dependent on the weather conditions (McMorrow, 2011). One large wildfire burn area occurred in the North-east of the Grampian Mountains in 2019 (see Figure 7a), covering 2224 ha of our study area, 25% of that year's burn total. However, such large fires are unusual. Our analysis identifies very few large fires with fires larger than 5 ha only accounting for only 10% of total burn area. Prior to 2009, and the introduction of the Incident Reporting System (IRS), there is limited standardised information about wildfire burnt area. Since 2009, and based on the Fire and Rescue Service IRS data, we estimate average annual wildfire burn areas on moorland in our study area of 800 ha, a small fraction of the total burn areas we are recording (ClimateXChange, n.d.; Gagkas et al., 2022). The data do show strong annual variability, and for our study area, our estimated wildfire burn area varied about twentyfold from 190 to 3500 ha. It has been estimated that over half of moorland burnt by wildfires may originate in prescribed fires that have escaped out of control (Holland et al., 2022; Worrall et al., 2010).

Prescribed burning occurs for a range of reasons including maintenance of grouse moor, or for improving grazing for livestock. We were unable to distinguish between burning for grouse shooting and burning for other purposes. Our map of burnt areas closely resembles mapping of grouse butt location (Matthews et al., 2020), suggesting that much of the burning is for grouse moor management. However, grass-dominated moor occurred in the west of the study area, especially the south-west of the Southern Uplands, interspersed with smaller areas that were heather dominated. Here, the burns were larger and more infrequent, and it is likely that burning here was done to improve grazing for deer and livestock. Conversely, grouse moor burning was characterised by groups of tight clusters of small burns although in these areas larger burns often occurred alongside these groups of smaller burns. The Muirburn Code advises burning in small patches or strips. We found about 80% of the burnt area was in small (<1 ha) burns, in line with the Muirburn code.

We made a preliminary assessment of the particulate air pollution emissions arising from muirburn. We estimate particulate emissions were similar to that emitted by road transport, suggesting that muirburn could have important negative impacts on air quality. We assumed that fires only burn above-ground vegetation and do not burn into peat soils. If fires burn peat soils, as can occur particularly in degraded peatlands, biomass consumption and PM emissions would increase substantially. Future studies are needed to assess the impacts of prescribed burning on air quality and public health.

Our study has a few issues that could be improved in future work. First, changes in NBR are caused by a range of disturbances to vegetation, such as hill-track construction, quarrying and construction work as well as natural disturbance events such as landslides, or erosion of peat hags. Nevertheless, our analysis of Google Earth

imagery (see Section 3.2.1) suggests that the majority of disturbance came from muirburn, with just 0.2% of classified burn area attributed to disturbance caused other than by burning. Sentinel-2 imagery, available after 2015 with higher temporal (10–20 m) and spatial (repeat period of 5 days) resolution, has already been exploited for burnt area mapping (Gaveau et al., 2021; Tanase et al., 2020) and should allow a better monitoring of muirburn in the future. Our verification section showed that our producer's accuracy was lower for smaller muirburns (Site 3), with accuracies that were generally about half that seen in sites with larger burn areas. Previous work in other regions (Gaveau et al., 2021) has found that burnt area detected by Sentinel-2 was double the estimate from Landsat. Higher resolution data will also allow analysis of the size of burns, fire return intervals and assessment of good burn practices such as avoiding water courses or steep slopes.

5 | CONCLUSIONS

We use a Landsat time series to estimate area burnt over eastern Scotland from 1985 to 2022, with NBR and variation in NBR used to detect burnt pixels. To the best of our knowledge, this is the first large-scale study to use Landsat imagery to quantitatively estimate area burnt over a long time series in the United Kingdom. We estimate an annual average burn area of 6100 ha, with substantial year-to-year variability. Our analysis suggests burning on deep peat is widespread, with 32% of total burn area on deep peat and no change in this fraction after a revised code of practise that advised against such burning was introduced in 2017. If the currently mooted Scottish legislation to tighten regulation of muirburning, including a prohibition on peatland burning, and the introduction of a compulsory licence for muirburns, is enacted, free, publicly available medium resolution Landsat and Sentinel imagery should be well placed to allow a thorough assessment of the implementation of these measures.

AUTHOR CONTRIBUTIONS

B. D. Spracklen conducted the analysis. B. D. Spracklen and D. V. Spracklen wrote the paper and discussed the work.

ACKNOWLEDGEMENTS

We thank Tomas Spracklen for his help in carrying out the fieldwork.

FUNDING INFORMATION

The research has been supported by funding from the European Research Council (ERC) under the European Union's Horizon 2020 research and innovation programme (DECAF project, Grant Agreement No. 771492) and the Natural Environment Research Council (NE/L013347/1).

CONFLICT OF INTEREST STATEMENT

The authors declare no conflicts of interest.

PEER REVIEW

The peer review history for this article is available at https://www.webofscience.com/api/gateway/wos/peer-review/10.1002/2688-8319.12296.

DATA AVAILABILITY STATEMENT

Publicly available datasets were analysed in this study. Landsat data can be found here: https://earthexplorer.usgs.gov/ (U.S. Geological Survey). Peatland extend can be found here: https://soils.environment.gov.scot/maps/thematic-maps/carbon-and-peatland-2016-map/ (Carbon and Peatland Map, 2016). Moorland extent can be found here: https://spatialdata.gov.scot/geonetwork/srv/api/records/88cea3bd-8679-48d8-8ffb-7d2f1182c175 (Habitat and Land Classification Map (HLCM), 2020).

ORCID

B. D. Spracklen https://orcid.org/0000-0001-9000-8804

D. V. Spracklen https://orcid.org/0000-0002-7551-4597

REFERENCES

Bain, C. G., Bonn, A., Stoneman, R., Chapman, S., Coupar, A., Evans, M., Gearey, B., Howat, M., Joosten, H., & Keenleyside, C. (2011). *IUCN UK Commission of Inquiry on Peatlands*. Published by the IUCN UK Peatland Programme.

Baines, D., Redpath, S., Richardson, M., & Thirgood, S. (2008). The direct and indirect effects of predation by Hen Harriers *Circus cyaneus* on trends in breeding birds on a Scottish grouse moor. *Ibis*, *150*, 27–36. https://doi.org/10.1111/j.1474-919x.2008.00848.x

Boschetti, L., Roy, D. P., Justice, C. O., & Humber, M. L. (2015). MODIS–Landsat fusion for large area 30 m burned area mapping. *Remote Sensing of Environment*, *161*, 27–42. https://doi.org/10.1016/j.rse.2015.01.022

Brown, L. E., & Holden, J. (2020). Contextualizing UK moorland burning studies with geographical variables and sponsor identity. *Journal of Applied Ecology*, *57*, 2121–2131. https://doi.org/10.1111/1365-2664.13708

Brown, L. E., Johnston, K., Palmer, S. M., Aspray, K. L., & Holden, J. (2013). River ecosystem response to prescribed vegetation burning on blanket peatland. *PLoS One*, *8*, e81023. https://doi.org/10.1371/journal.pone.0081023

Carbon and Peatland Map. (2016). https://soils.environment.gov.scot/maps/thematic-maps/carbon-and-peatland-2016-map/

Chapman, S. J., Bell, J., Donnelly, D., & Lilly, A. (2009). Carbon stocks in Scottish peatlands. *Soil Use and Management*, *25*, 105–112. https://doi.org/10.1111/j.1475-2743.2009.00219.x

Clay, G. D., Worrall, F., & Aebischer, N. J. (2012). Does prescribed burning on peat soils influence DOC concentrations in soil and runoff waters? Results from a 10 year chronosequence. *Journal of Hydrology*, *448*, 139–148. https://doi.org/10.1016/j.jhydrol.2012.04.048

ClimateXChange. (n.d.). Number and area of reported wildfires in forests and key habitats. https://www.climatexchange.org.uk/research/indicators-and-trends/indicators/nb42-nf1718-number-and-area-of-reported-wildfires-in-forests-and-key-habitats/

Crowle, A. J., Glaves, D. J., Oakley, N., Drewitt, A. L., & Denmark-Melvin, M. E. (2022). Alternative future land use options in the British uplands. https://doi.org/10.1111/ibi.13041

Davies, G. M., Hamilton, A., Smith, A., & Legg, C. J. (2008). Using visual obstruction to estimate heathland fuel load and structure. *International Journal of Wildland Fire*, *17*, 380–389. https://doi.org/10.1071/wf07021

Davies, G. M., Kettridge, N., Stoof, C. R., Gray, A., Ascoli, D., Fernandes, P. M., Marrs, R., Allen, K. A., Doerr, S. H., & Clay, G. D. (2016). The role of fire in UK peatland and moorland management: The need for informed, unbiased debate. *Philosophical Transactions of the Royal Society B: Biological Sciences*, *371*, 20150342. https://doi.org/10.1098/rstb.2015.0342

de Bem, P. P., de Carvalho Júnior, O. A., de Carvalho, O. L. F., Gomes, R. A. T., & Fontes Guimarães, R. (2020). Performance analysis of deep convolutional autoencoders with different patch sizes for change detection from burnt areas. *Remote Sensing*, *12*, 2576. https://doi.org/10.3390/rs12162576

Douglas, D. J., Buchanan, G. M., Thompson, P., Amar, A., Fielding, D. A., Redpath, S. M., & Wilson, J. D. (2016). Vegetation burning for game management in the UK uplands is increasing and overlaps spatially with soil carbon and protected areas. *Biological Conservation*, *191*, 243–250. https://doi.org/10.1016/j.biocon.2016.01.002

Evans, C. D., Peacock, M., Baird, A. J., Artz, R. R. E., Burden, A., Callaghan, N., Chapman, P. J., Cooper, H. M., Coyle, M., & Craig, E. (2021). Overriding water table control on managed peatland greenhouse gas emissions. *Nature*, *593*, 548–552. https://doi.org/10.1038/s41586-021-03523-1

Friedlingstein, P., O'sullivan, M., Jones, M. W., Andrew, R. M., Gregor, L., Hauck, J., Le Quéré, C., Luijkx, I. T., Olsen, A., Peters, G. P., Peters, W., Pongratz, J., Schwingshackl, C., Sitch, S., Canadell, J. G., Ciais, P., Jackson, R. B., Alin, S. R., Alkama, R., … Zheng, B. (2022). Global carbon budget 2022. *Earth System Science Data Discussions*, *2022*, 1–159.

Fuller, R., & Calladine, J. (2014). Landscape transition through natural processes: Implications for biodiversity of tree regeneration on moorland. In *Proceedings of the ecology and conservation of birds in upland and alpine habitats* (pp. 896–900). Proceedings of the BOU Annual Conference.

Gagkas, Z., Campbell, G., Owen, J., & Davies, M. (2022). *Provision of analyses of Scottish fire and rescue service (SFRS) incident reporting system (IRS) data in relation to wildfire incidents*. The James Hutton Institute https://www.gov.scot/binaries/content/documents/govscot/publications/research-and-analysis/2022/03/provision-analyses-scottish-fire-rescue-service-sfrs-incident-reporting-system-irs-data-relation-wildfire-incidents/documents/provision-analyses-scottish-fire-rescue-service-sfrs-incident-reporting-system-irs-data-relation-wildfire-incidents/provision-analyses-scottish-fire-rescue-service-sfrs-incident-reporting-system-irs-data-relation-wildfire-incidents/govscot%3Adocument/provision-analyses-scottish-fire-rescue-service-sfrs-incident-reporting-system-irs-data-relation-wildfire-incidents.pdf

Gallego-Sala, A. V., Clark, J. M., House, J. I., Orr, H. G., Prentice, I. C., Smith, P., & Chapman, S. J. (2010). Bioclimatic envelope model of climate change impacts on blanket peatland distribution in Great Britain. *Climate Research*, *45*, 151–162. https://doi.org/10.3354/cr00911

Garnett, M. H., Ineson, P., & Stevenson, A. C. (2000). Effects of burning and grazing on carbon sequestration in a Pennine blanket bog, UK. *The Holocene*, *10*, 729–736. https://doi.org/10.1191/095968300094971

Gaveau, D. L., Descals, A., Salim, M. A., Sheil, D., & Sloan, S. (2021). Refined burned-area mapping protocol using Sentinel-2 data increases estimate of 2019 Indonesian burning. *Earth System Science Data*, *13*, 5353–5368. https://doi.org/10.5194/essd-13-5353-2021

Glaves, D. J., Crowle, A. J. W., Bruemmer, C., & Lenaghan, S. A. (2020). The causes and prevention of wildfire on heathlands and peatlands in England (NEER014). *Natural England Evidence Review*, 43. https://publications.naturalengland.org.uk/publication/4741162353295360

Graham, A. M., Pope, R. J., McQuaid, J. B., Pringle, K. P., Arnold, S. R., Bruno, A. G., Moore, D. P., Harrison, J. J., Chipperfield, M. P., & Rigby, R. (2020). Impact of the June 2018 Saddleworth Moor wildfires on air quality in northern England. *Environmental Research Communications*, *2*, 031001. https://doi.org/10.5194/egusphere-egu2020-8290

Graham, A. M., Pope, R. J., Pringle, K. P., Arnold, S., Chipperfield, M. P., Conibear, L. A., Butt, E. W., Kiely, L., Knote, C., & McQuaid, J. B. (2020). Impact on air quality and health due to the Saddleworth moor fire in northern England. *Environmental Research Letters*, *15*, 074018.

Greenpeace. (2022). Satellites reveal widespread burning on England's protected peatlands, despite government ban. https://unearthed.greenpeace.org/2022/05/30/satellites-fires-burning-england-peatland-grouse-shooting/

Habitat and Land Classification Map (HLCM). (2020). https://spatialdata.gov.scot/geonetwork/srv/api/records/88cea3bd-8679-48d8-8ffb-7d2f1182c175

Harper, A. R., Doerr, S. H., Santin, C., Froyd, C. A., & Sinnadurai, P. (2018). Prescribed fire and its impacts on ecosystem services in the UK. *Science of the Total Environment*, *624*, 691–703. https://doi.org/10.1016/j.scitotenv.2017.12.161

Hester, A. J., Miller, D. R., & Towers, W. (1996). Landscape-scale vegetation change in the Cairngorms, Scotland, 1946-1988: Implications for land management. *Biological Conservation*, *77*, 41–51. https://doi.org/10.1016/0006-3207(96)80650-1

Hester, A. J., & Sydes, C. (1992). Changes in burning of Scottish heather moorland since the 1940s from aerial photographs. *Biological Conservation*, *60*, 25–30. https://doi.org/10.1016/0006-3207(92)90795-o

Holden, J., Chapman, P. J., & Labadz, J. C. (2004). Artificial drainage of peatlands: Hydrological and hydrochemical process and wetland restoration. *Progress in Physical Geography*, *28*, 95–123. https://doi.org/10.1191/0309133304pp403ra

Holden, J., Palmer, S. M., Johnston, K., Wearing, C., Irvine, B., & Brown, L. E. (2015). Impact of prescribed burning on blanket peat hydrology. *Water Resources Research*, *51*, 6472–6484. https://doi.org/10.1002/2014wr016782

Holden, J., Shotbolt, L., Bonn, A., Burt, T. P., Chapman, P. J., Dougill, A. J., Fraser, E. D. G., Hubacek, K., Irvine, B., & Kirkby, M. J. (2007). Environmental change in moorland landscapes. *Earth-Science Reviews*, *82*, 75–100. https://doi.org/10.1016/j.earscirev.2007.01.003

Holden, J., Wearing, C., Palmer, S., Jackson, B., Johnston, K., & Brown, L. E. (2014). Fire decreases near-surface hydraulic conductivity and macropore flow in blanket peat. *Hydrological Processes*, *28*, 2868–2876. https://doi.org/10.1002/hyp.9875

Holland, J. P., Polloc, M., Buckingham, S., Glendinning, J., & McCracken, D. (2022). *Reviewing, assessing and critiquing the evidence base on the impacts of muirburn on wildfire prevention, carbon storageand biodiversity*. NatureScot Research Report 1302 https://pure.sruc.ac.uk/ws/portalfiles/portal/54385017/nature.scot_NatureScot_Research_Report_1302_Reviewing_assessing_and_critiquing_the_evidence_base_on_the_impacts.pdf

Hollis, D., McCarthy, M., Kendon, M., Legg, T., & Simpson, I. (2019). HadUK-Grid-A new UK dataset of gridded climate observations. *Geoscience Data Journal*, *6*(2), 151–159.

Hoo, Z. H., Candlish, J., & Teare, D. (2017). What is an ROC curve? *Emergency Medecine Journal*, *34*(6), 357–359. https://doi.org/10.1136/emermed-2017-206735

Jarvis, A., Reuter, H. I., Nelson, A., & Guevara, E. (2008). Hole-filled SRTM for the globe version 4.

Leroy, A. M., & Rousseeuw, P. J. (1987). *Robust regression and outlier detection* (1st ed.). John Wiley and Sons.

Li, C., Grayson, R., Holden, J., & Li, P. (2018). Erosion in peatlands: Recent research progress and future directions. *Earth-Science*

Reviews, *185*, 870–886. https://doi.org/10.1016/j.earscirev.2018.08.005

Littlewood, N. A., Mason, T. H., Hughes, M., Jaques, R., Whittingham, M. J., & Willis, S. G. (2019). The influence of different aspects of grouse moorland management on nontarget bird assemblages. *Ecology and Evolution*, *9*, 11089–11101. https://doi.org/10.1002/ece3.5613

Ludwig, S. C., Roos, S., & Baines, D. (2019). Responses of breeding waders to restoration of grouse management on a moor in South-West Scotland. *Journal of Ornithology*, *160*, 789–797. https://doi.org/10.1007/s10336-019-01667-6

Mancino, G., Ferrara, A., Padula, A., & Nole, A. (2020). Cross-comparison between Landsat 8 (OLI) and Landsat 7 (ETM+) derived vegetation indices in a mediterranean environment. *Remote Sensing*, *12*, 291. https://doi.org/10.3390/rs12020291

Marrs, R. H., Marsland, E.-L., Lingard, R., Appleby, P. G., Piliposyan, G. T., Rose, R. J., O'Reilly, J., Milligan, G., Allen, K. A., & Alday, J. G. (2019). Experimental evidence for sustained carbon sequestration in fire-managed, peat moorlands. *Nature Geoscience*, *12*, 108–112. https://doi.org/10.1038/s41561-018-0266-6

Martin-Ortega, J., Allott, T. E., Glenk, K., & Schaafsma, M. (2014). Valuing water quality improvements from peatland restoration: Evidence and challenges. *Ecosystem Services*, *9*, 34–43. https://doi.org/10.1016/j.ecoser.2014.06.007

Matthews, K., Fielding, D., Miller, D., Gandossi, G., Newey, S., & Thomson, S. G. (2020). Mapping the areas of moorland that are actively managed for grouse and the intensity of current management regimes: Part 3–research to assess socioeconomic and biodiversity impacts of driven grouse moors and to understand the rights of gamekeepers.

McMorrow, J. (2011). Wildfire in the United Kingdom: Status and key issues. In *Proceedings of the Second International Association of Wildland Fire Conference on human dimensions of wildland fire* (pp. 44–56). International Association of Wildland Fire.

Miller, G. R. (1980). The burning of heather moorland for red grouse. *Bulletin of Ecology*, *11*, 725–733.

Miller, J. D., & Thode, A. E. (2007). Quantifying burn severity in a heterogeneous landscape with a relative version of the delta Normalized Burn Ratio (dNBR). *Remote Sensing of Environment*, *109*, 66–80. https://doi.org/10.1016/j.rse.2006.12.006

Nature England, & Glaves, D. (2013). *The effects of managed burning on upland peatland biodiversity, carbon and water*. Natural England.

Newey, S., Mustin, K., Bryce, R., Fielding, D., Redpath, S., Bunnefeld, N., Daniel, B., & Irvine, R. J. (2016). Impact of management on avian communities in the Scottish highlands. *PLoS One*, *11*, e0155473. https://doi.org/10.1371/journal.pone.0155473

Noble, A., Crowle, A., Glaves, D. J., Palmer, S. M., & Holden, J. (2019). Fire temperatures and sphagnum damage during prescribed burning on peatlands. *Ecological Indicators*, *103*, 471–478. https://doi.org/10.1016/j.ecolind.2019.04.044

Noble, A., Palmer, S. M., Glaves, D. J., Crowle, A., Brown, L. E., & Holden, J. (2018). Prescribed burning, atmospheric pollution and grazing effects on peatland vegetation composition. *Journal of Applied Ecology*, *55*, 559–569. https://doi.org/10.1111/1365-2664.12994

Parks, S. A., Dillon, G. K., & Miller, C. (2014). A new metric for quantifying burn severity: The relativized burn ratio. *Remote Sensing*, *6*, 1827–1844. https://doi.org/10.3390/rs6031827

Parry, L. E., Holden, J., & Chapman, P. J. (2014). Restoration of blanket peatlands. *Journal of Environmental Management*, *133*, 193–205. https://doi.org/10.1016/j.jenvman.2013.11.033

Ramchunder, S. J., Brown, L. E., & Holden, J. (2012). Catchment-scale peatland restoration benefits stream ecosystem biodiversity. *Journal of Applied Ecology*, *49*, 182–191. https://doi.org/10.1111/j.1365-2664.2011.02075.x

Ramchunder, S. J., Brown, L. E., & Holden, J. (2013). Rotational vegetation burning effects on peatland stream ecosystems. *Journal of Applied Ecology*, *50*, 636–648. https://doi.org/10.1111/1365-2664.12082

Ramo, R., Roteta, E., Bistinas, I., Van Wees, D., Bastarrika, A., Chuvieco, E., & Van der Werf, G. R. (2021). African burned area and fire carbon emissions are strongly impacted by small fires undetected by coarse resolution satellite data. *Proceedings of the National Academy of Sciences of the United States of America*, *118*, e2011160118. https://doi.org/10.1073/pnas.2011160118

Robertson, P. A., Park, K. J., & Barton, A. F. (2001). Loss of heather *Calluna vulgaris* moorland in the Scottish uplands: The role of red grouse *Lagopus lagopus* scoticus management. *Wildlife Biology*, *7*, 11–16. https://doi.org/10.2981/wlb.2001.004

Roteta, E., Bastarrika, A., Ibisate, A., & Chuvieco, E. (2021). A preliminary global automatic burned-area algorithm at medium resolution in Google Earth Engine. *Remote Sensing*, *13*, 4298. https://doi.org/10.3390/rs13214298

Roteta, E., Bastarrika, A., Padilla, M., Storm, T., & Chuvieco, E. (2019). Development of a Sentinel-2 burned area algorithm: Generation of a small fire database for sub-Saharan Africa. *Remote Sensing of Environment*, *222*, 1–17. https://doi.org/10.1016/j.rse.2018.12.011

Roy, D. P., Huang, H., Boschetti, L., Giglio, L., Yan, L., Zhang, H. H., & Li, Z. (2019). Landsat-8 and Sentinel-2 burned area mapping-a combined sensor multi-temporal change detection approach. *Remote Sensing of Environment*, *231*, 111254. https://doi.org/10.1016/j.rse.2019.111254

RSPB. (2023). Upland burning. https://upland-burning-rspb.hub.arcgis.com/

Santana, N. C., de Carvalho Júnior, O. A., Gomes, R. A. T., & Guimarães, R. F. (2018). Burned-area detection in Amazonian environments using standardized time series per pixel in MODIS data. *Remote Sensing*, *10*, 1904. https://doi.org/10.3390/rs10121904

ScotGov. (2023). Wildlife Management and Muirburn (Scotland) Bill Policy Memorandum. https://www.parliament.scot/-/media/files/legislation/bills/s6-bills/wildlife-management-and-muirburn-scotland-bill/introduced/policy-memorandum.pdf

Smith, P., Smith, J. U., Flynn, H., Killham, K., Rangel-Castro, I., Foereid, B., Aitkenhead, M., Chapman, S., Towers, W., Bell, J., Lumsdon, D., Milne, R., Thomson, A., Simmons, I., Skiba, U., Reynolds, B., Evans, C., Frogbrook, Z., Bradley, I., … Falloon, P. (2007). *ECOSSE: Estimating carbon in organic soils—Sequestration and emissions* (Final Report, 166 pp.). SEERAD Report. ISBN 978 0 7559 1498 2.

Tanase, M. A., Belenguer-Plomer, M. A., Roteta, E., Bastarrika, A., Wheeler, J., Fernández-Carrillo, Á., Tansey, K., Wiedemann, W., Navratil, P., & Lohberger, S. (2020). Burned area detection and mapping: Intercomparison of Sentinel-1 and Sentinel-2 based algorithms over tropical Africa. *Remote Sensing*, *12*, 334. https://doi.org/10.3390/rs12020334

Tharme, A. P., Green, R. E., Baines, D., Bainbridge, I. P., & O'Brien, M. (2001). The effect of management for red grouse shooting on the population density of breeding birds on heather-dominated moorland. *Journal of Applied Ecology*, *38*, 439–457. https://doi.org/10.1046/j.1365-2664.2001.00597.x

Thompson, P. S., Douglas, D. J., Hoccom, D. G., Knott, J., Roos, S., & Wilson, J. D. (2016). Environmental impacts of high-output driven shooting of Red Grouse *Lagopus lagopus scotica*. *Ibis*, *158*, 446–452. https://doi.org/10.1111/ibi.12356

Transport Scotland (2018). *Chapter 13: Environment and emissions*. Transport Scotland. https://www.transport.gov.scot/publication/scottish-transport-statistics-no-37-2018-edition/chapter-13-environment-and-emissions/

U.S. Geological Survey Landsat collection 2 level 2. https://earthexplorer.usgs.gov

UKGov. (2021). Heather and grass burning regulations. https://www.legislation.gov.uk/uksi/2021/158/made/data.pdf

Vetrita, Y., Cochrane, M. A., Priyatna, M., Sukowati, K. A., & Khomarudin, M. R. (2021). Evaluating accuracy of four MODIS-derived burned area products for tropical peatland and non-peatland fires. *Environmental Research Letters*, *16*(3), 035015. https://doi.org/10.1088/1748-9326/abd3d1

Wallage, Z. E., Holden, J., & McDonald, A. T. (2006). Drain blocking: An effective treatment for reducing dissolved organic carbon loss and water discolouration in a drained peatland. *Science of the Total Environment*, *367*, 811–821. https://doi.org/10.1016/j.scitotenv.2006.02.010

Ward, S. E., Bardgett, R. D., McNamara, N. P., Adamson, J. K., & Ostle, N. J. (2007). Long-term consequences of grazing and burning on northern peatland carbon dynamics. *Ecosystems*, *10*, 1069–1083. https://doi.org/10.1007/s10021-007-9080-5

Wiedinmyer, C., Akagi, S. K., Yokelson, R. J., Emmons, L. K., Al-Saadi, J. A., Orlando, J. J., & Soja, A. J. (2011). The fire inventory from NCAR (FINN): A high resolution global model to estimate the emissions from open burning. *Geoscientific Model Development*, *4*, 625–641. https://doi.org/10.5194/gmd-4-625-2011

Worrall, F., Armstrong, A., & Holden, J. (2007). Short-term impact of peat drain-blocking on water colour, dissolved organic carbon concentration, and water table depth. *Journal of Hydrology*, *337*, 315–325. https://doi.org/10.1016/j.jhydrol.2007.01.046

Worrall, F., Chapman, P., Holden, J., Evans, C., Artz, R., Smith, P., & Grayson, R. (2011). A review of current evidence on carbon fluxes and greenhouse gas emissions from UK peatland. JNCC Report, No. 442.

Worrall, F., Clay, G. D., Marrs, R., & Reed, M. S. (2010). *Impacts of burning management on peatlands* Scientific review, 2011. IUCN Peatland Programme.

Yallop, A. R., Thacker, J. I., Thomas, G., Stephens, M., Clutterbuck, B., Brewer, T., & Sannier, C. A. D. (2006). The extent and intensity of management burning in the English uplands. *Journal of Applied Ecology*, *43*, 1138–1148. https://doi.org/10.1111/j.1365-2664.2006.01222.x

SUPPORTING INFORMATION

Additional supporting information can be found online in the Supporting Information section at the end of this article.

Figure S1. Deep peat areas in (a) northern study area and (b) southern study area.

Figure S2. Percentage of pixels across our study area that are not obscured by cloud, cloud shadow, snow or sensor malfunction.

Figure S3. This figure shows for each Landsat pixel how many years are clear (unobscured by snow, cloud, cloud shadow or sensor malfunction) for (a) northern study area and (b) southern study area. There are 39 years in our time-series analysis, covering 1984 to 2022 inclusive. Therefore, the maximum value is 39, for a pixel which was clear every single year of our analysis.

Figure S4. True positive rate (TPR) plotted against false positive rate (FPR; both adjusted for site burn area) for a range of ΔNBR thresholds, calculated over (a) six calibration sites and (b) six accuracy assessment sites and two field sites, for fractional pixel classification (Equation 12) and binary pixel classification.

Figure S5. Burnt pixels for the northern study area grouped into seven periods.

Figure S6. Burnt pixels for the southern study area grouped into seven periods.

Table S1. Site 1 Year 2020: User's accuracy of 77.1% and producer's accuracy of 60.2% for burnt areas.

Table S2. Site 1 Year 2019: User's accuracy of 99.8% and producer's accuracy of 82.1% for burnt areas.

Table S3. Site 2 Year 2019: User's accuracy of 97.5% and producer's accuracy of 92.4% for burnt areas.

Table S4. Site 2 Year 2018: User's accuracy of 96.7% and producer's accuracy of 84.4% for burnt areas.

Table S5. Site 2 Year 2017: User's accuracy of 40.5% and producer's accuracy of 75.8% for burnt areas.

Table S6. Site 3 Year 2018: User's accuracy of 59.6% and producer's accuracy of 31.7% for burnt areas.

Table S7. Site 3 Year 2017: User's accuracy of 86.5% and producer's accuracy of 36.7% for burnt areas.

Table S8. Site 3 Year 2016: User's accuracy of 85.7% and producer's accuracy of 67.7% for burnt areas.

Table S9. Site 4: User's accuracy of 91% and producer's accuracy of 70.1% for burnt areas.

Table S10. Site 5: User's accuracy of 27.8% and producer's accuracy of 58.3% for burnt areas.

Table S11. Site 6 Year 2021: User's accuracy of 68.5% and producer's accuracy of 93.7% for burnt areas.

Table S12. Site 6 Year 2020: User's accuracy of 92% and producer's accuracy of 89.4% for burnt areas.

Table S13. Site 6 Year 2019: User's accuracy of 98.9% and producer's accuracy of 73.2% for burnt areas.

Table S14. Field Study Site 1: User's accuracy of 100% and producer's accuracy of 40% for burnt areas.

Table S15. Field Study Site 2: User's accuracy of 99.4% and producer's accuracy of 92.7% for burnt areas.

How to cite this article: Spracklen, B. D., & Spracklen, D. V. (2023). Assessment of peatland burning in Scotland during 1985–2022 using Landsat imagery. *Ecological Solutions and Evidence*, *4*, e12296. https://doi.org/10.1002/2688-8319.12296